

1 Supporting Information for:

2 Improving understanding of operational conditions for oxidant application 3 during NOM and manganese treatment.

4 Chu X.,¹ Agostino A.,¹ Rao N.R.H.,¹ Moradi S.,^{1,a} Bustamante H.,² Power K.,² Henderson
5 R.K.,¹ Leslie G.L.¹

6 ¹ School of Chemical Engineering, The University of New South Wales, Sydney, NSW
7 2052, Australia

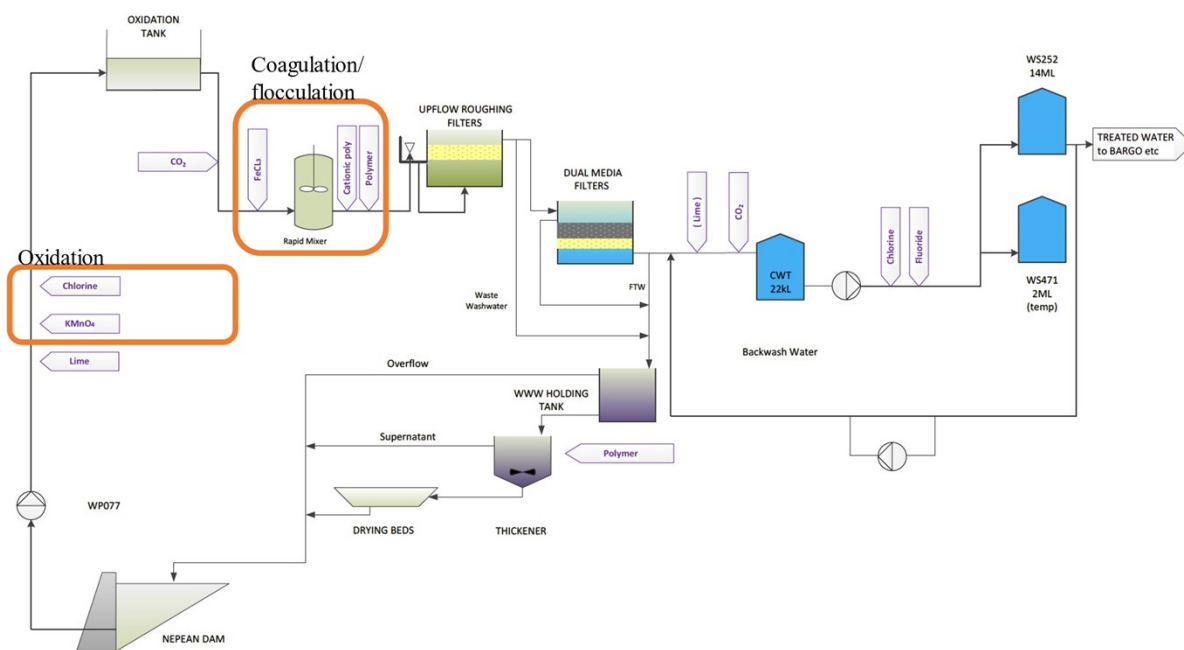
8 ² Sydney Water, 1 Smith Street, Parramatta NSW 2125, Australia

9 ^a Artificial Intelligence Centre of Excellence (AI CoE), NCS Group, Sydney, NSW, 2113,
10 Australia

11 * Corresponding author – g.leslie@unsw.edu.au

12 1. Materials and methods

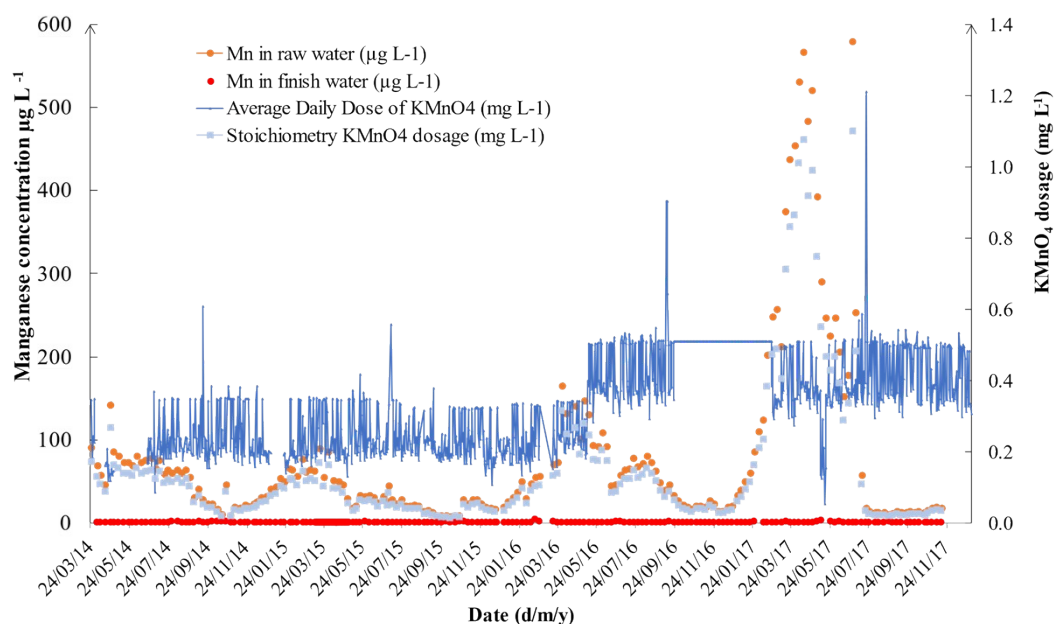
13 1.1 Nepean Water Filtration Plant (WFP) process flow diagram



15 Fig. S1. Nepean WTP process flow diagram with oxidation and coagulation/flocculation
16 processes circled.

17 1.2 Historical data of Nepean WTP

18 Historical data of manganese concentration in the raw and finished water; and the KMnO_4
19 doses in the treatment plant was plotted in **Fig. S2**. (Data from Sydney Water Corporation.)



20

21 Fig. S2. Historical data for the manganese concentrations in the raw and finished water; the
22 potassium permanganate dose in the WTP and the calculated stoichiometric KMnO_4 dosages
23 relative to raw manganese concentration.

24 From March 2014 to December 2017, the manganese concentration fluctuated at a level below
25 $100 \mu\text{g L}^{-1}$ with peaks every March to May. In April 2017, the manganese concentration in raw
26 water peaked at around $500 \mu\text{g L}^{-1}$, followed by a dramatic drop back to a normal value below
27 $100 \mu\text{g L}^{-1}$. However, despite the fluctuation of the manganese level in the feed water, the dose
28 of KMnO_4 used in the treatment process remained stable, with only one increase from
29 approximately 0.3 to 0.5 mg L^{-1} and for most of the time the dose was higher than what was
30 stoichiometrically required to remove manganese (**Fig. S2**). Nevertheless, the manganese
31 concentrations in the finished water were always maintained at desirable values below $30 \mu\text{g}$
32 L^{-1} (guideline= 0.05 mg L^{-1} (1–3) even with the most extreme scenario in April 2017. This
33 indicated the KMnO_4 treatment had successfully reacted with and removed almost all the
34 manganese in water despite the doses being overdose or underdose. From the perspective of
35 DWTP, lower manganese concentrations mean less taste and odour problems or less potential
36 damage on the pipelines.

37 1.3 Liquid chromatography-organic carbon detection

38 Within the LC-OCD system, a weak cation exchange size-exclusion column on basis of
39 polymethacrylate was coupled (250 mm x 20 mm, Toyopearl TSK HW 50S, Tosoh Bioscience,
40 Japan). The mobile phase of phosphate buffer solution (2.5 g L⁻¹ KH₂PO₄ and 1.5 g L⁻¹
41 Na₂HPO₄·2H₂O) of pH 6.85 operates at flow rate of 1.1 mL min⁻¹. Injection volume was set
42 at 1 mL. Potassium hydrogen phthalate and potassium nitrate were used for OCD and OND
43 detector calibration, respectively. Humic substance molecular weights were calibrated using
44 Suwannee River standard II humic (HA) and fulvic acids (FA) from International Humic
45 Substances Society (IHSS). The average molecular weights for IHSS-FA and IHSS-HA
46 molecular weights were determined to be 711 and 1066 Da, respectively. Result integration
47 was processed on the ChromCalc software (DOC-Labor, Germany). LC-OCD fractionates
48 NOM to biopolymers, humic substances, building blocks, low molecular weight neutrals
49 (LMWN) and low molecular weight acids (LMWA) accordingly. More detailed analysis had
50 been previously described by Huber et al., (2011) (5).

51 1.4 Fluorescence EEMs

52 Five common excitation/emission peaks were defined for marine and terrestrial DOM: humic-
53 like **Peak A** ($\lambda_{ex/em} = 260/380 - 460nm$); humic-like **Peak C** ($\lambda_{ex/em} = 350/420 - 480nm$); marine
54 humic-like **Peak M** ($\lambda_{ex/em} = 312/380 - 420nm$); tyrosine-like, protein-like **Peak B** (
55 $\lambda_{ex/em} = 275/310nm$); tryptophan-like, protein-like **Peak T** ($\lambda_{ex/em} = 275/340nm$).

56 1.5 Floc strength and breakage model

57 The floc strength co-efficient log (C) value depends on the floc size measurement so that the
58 results could only be compared within the same experiment setup. The stable floc size exponent
59 ν value could be determined from the slope of the model and it represented the floc breakage
60 pattern with increasing shear forces. Parker et al., (1972) suggested that floc breakage was
61 dominated by floc fragmentation when ν remained 0.5, whilst erosion mechanisms dominated
62 with $\nu = 1$, and $\nu = 2$ suggested surface erosion breakage (6).

63 Table S1. Average velocity gradient (shear rate) (s⁻¹) under different impeller stirring speed.

64 Data under 22 °C was used for this study.

Speed [RPM]	Velocity gradients (s ⁻¹)	
	Temperature (°C)	
	20	22
10	3.5	3.6
20	10.0	10.3

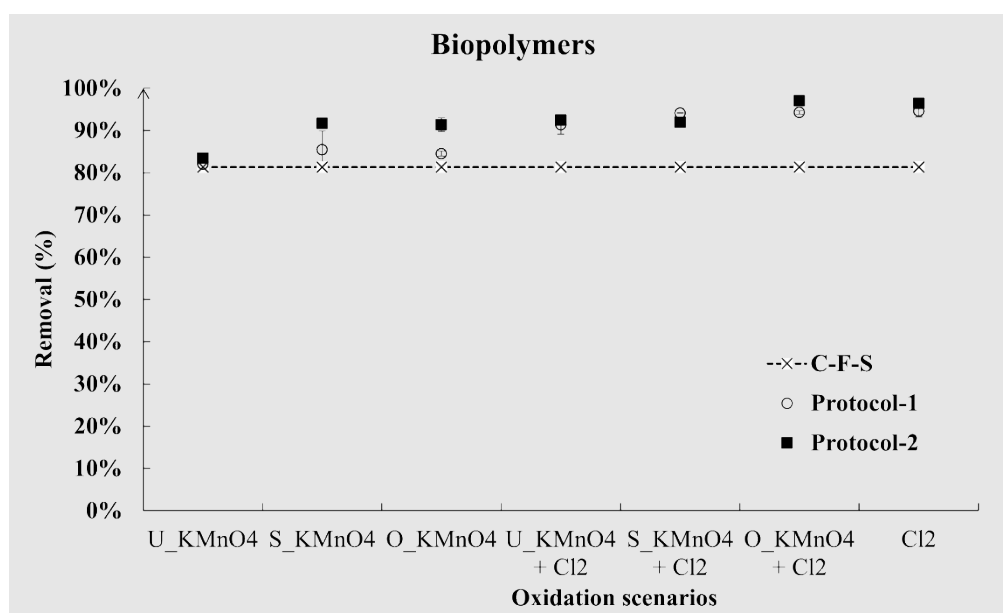
30	18.4	18.8
40	28.3	29.0
50	39.6	40.5
60	52.0	53.5
70	65.5	67.1
80	80.1	82.0
90	95.5	97.9
100	111.9	114.6
110	129.1	132.2
120	147.1	150.7
130	165.8	169.9
140	185.3	189.9
150	205.5	210.6
160	226.4	232.0
170	248.0	254.1
180	270.2	276.3
190	193.0	300.2
200	316.4	324.2

65

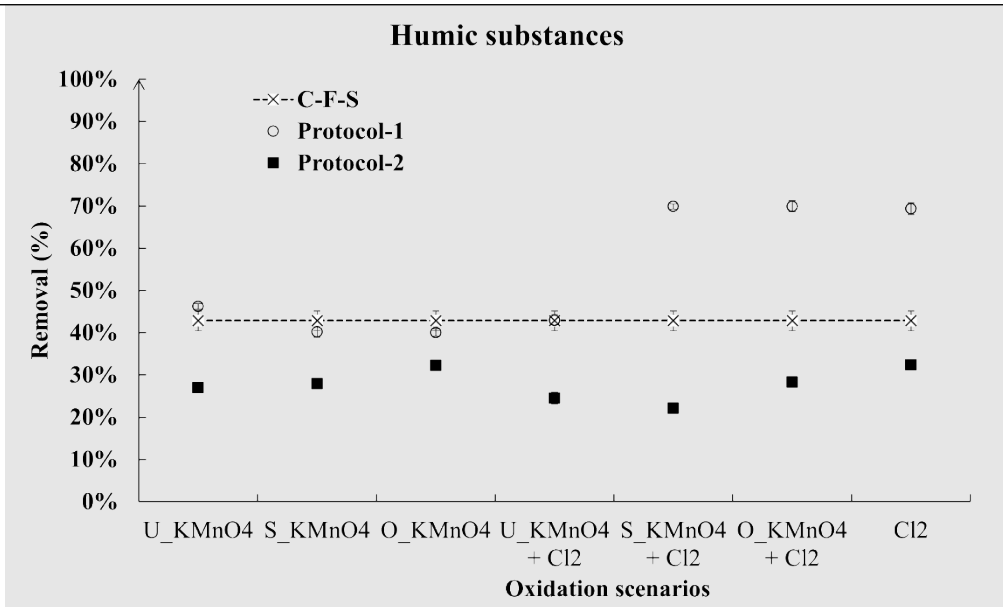
66 2. Results

67 2.1 NOM characterisation using liquid chromatography – organic carbon detection

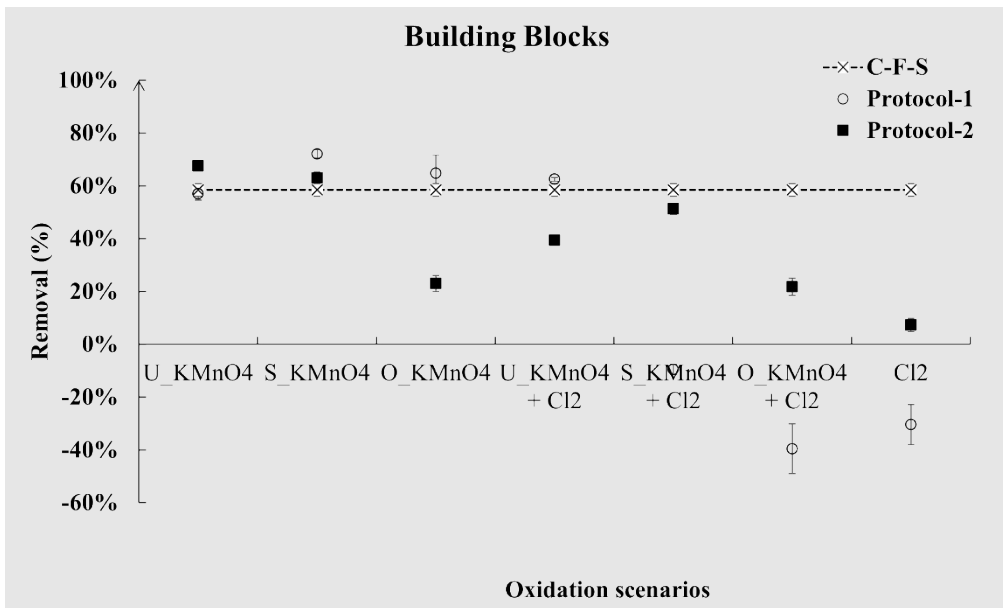
(a)



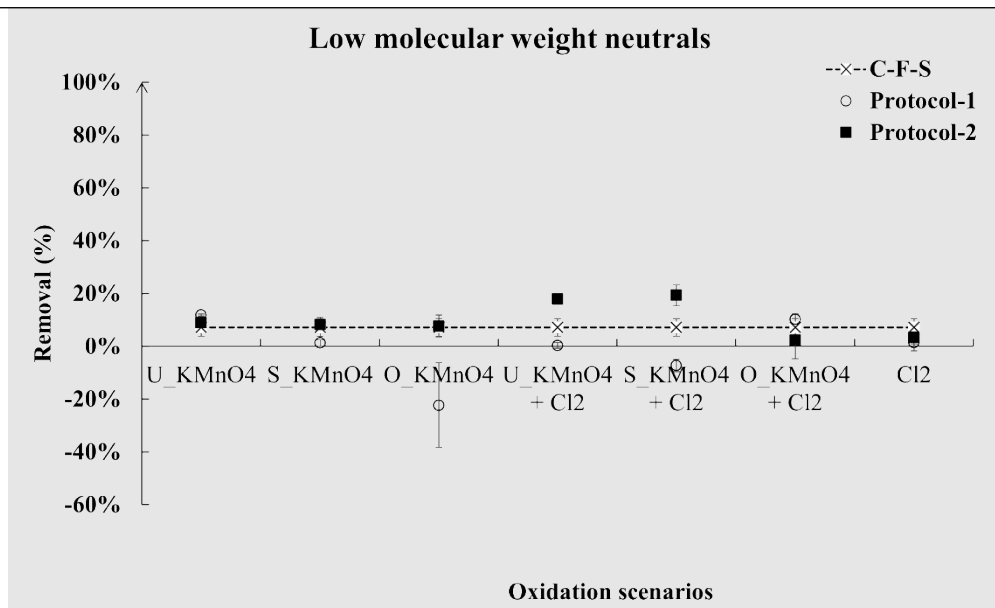
(b)



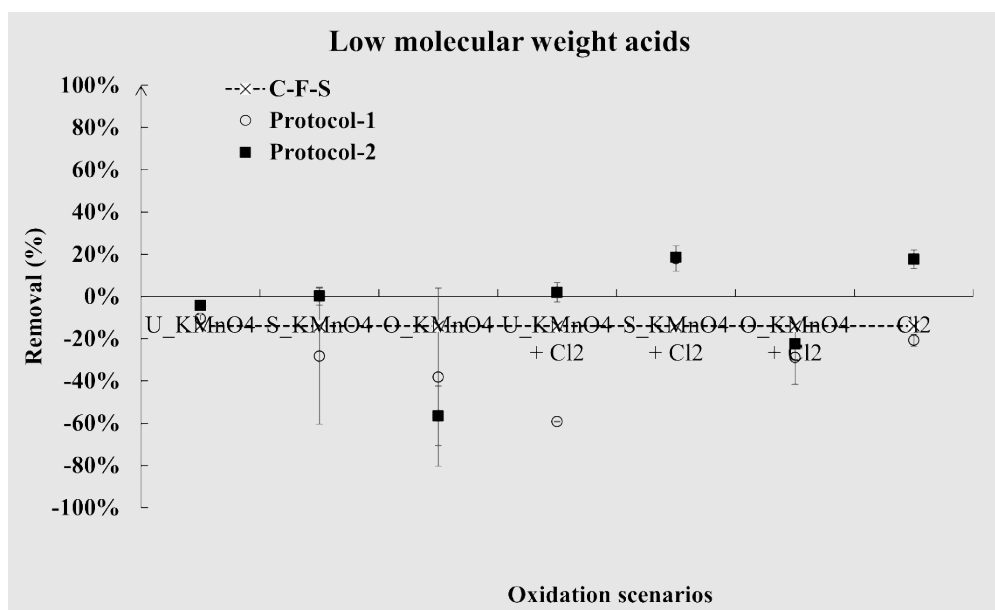
(c)



(d)

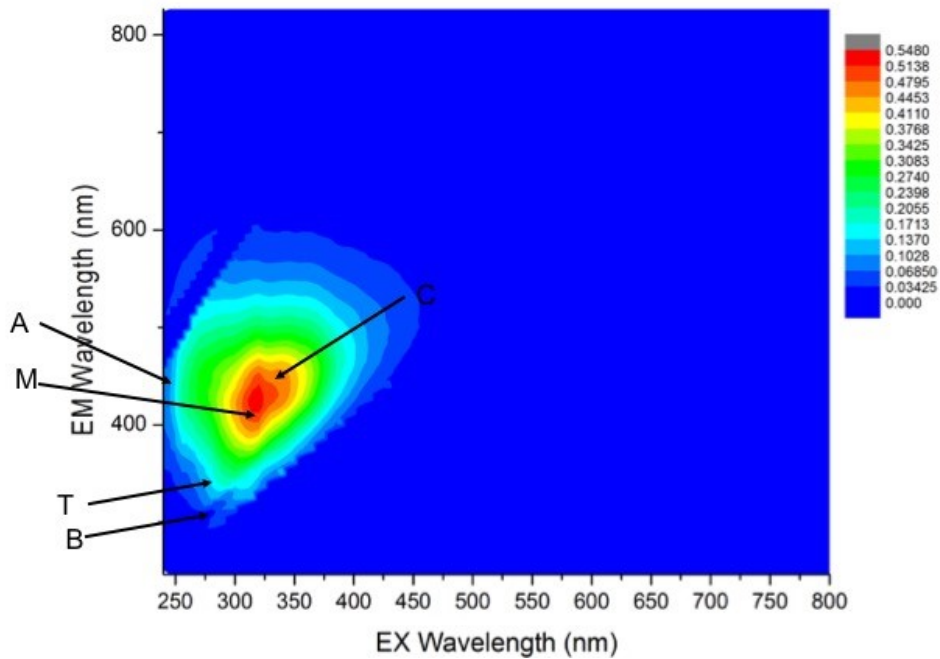


(e)



68 Fig. S3. Fraction concentrations from LC-OCD for coagulation, pre-oxidation enhanced
 69 coagulation and post-oxidation after coagulation: (a) Biopolymer; (b) Humic substances; (c)
 70 Building blocks, (d) LMWN, (e) LMWA.

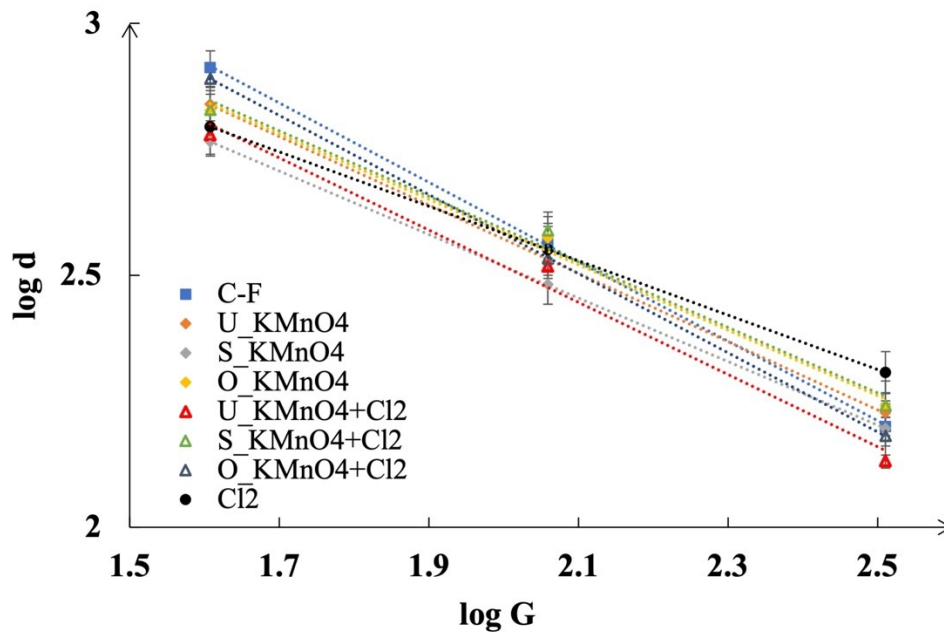
71 **2.2 NOM characterisation using fluorescence excitation-emission matrices**



72

73 Fig. S4. Fluorescence EEM contour plot for the feed water with fluorescence peak A, B, C, M,
74 T locations.

75 **2.3 Floc breakage model**

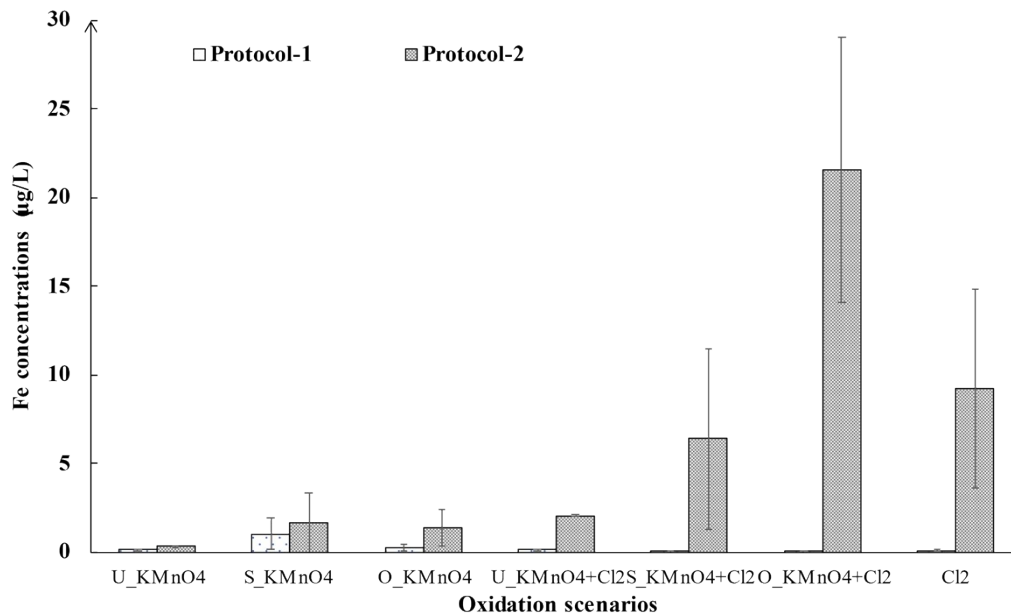


76

77 Fig. S5. Linear correlation of $\log(d)$ (steady floc size) and $\log(G)$ (shear rate) for the flocs
78 generated from the seven oxidation scenarios in Protocol-1, and only C-F in Protocol-2.

79 From the empirical expression suggested by Parker et al., (1972), the floc strength co-efficient
 80 C , and stable floc size exponent γ could be derived from linearization of \log (steady floc size)
 81 and \log (shear rate) (6). The shear rates of jar tester employed in this study were provided by
 82 the Platypus Jar Tester manufacturer. From **Fig. S5**, differences in the slopes and intercepts
 83 with y-axis were minor, indicating the different pre-oxidation scenarios did not vary floc
 84 breakage pattern or floc strength much.

85 2.4 Iron removal



86

87 Fig. S6. Residual soluble iron concentration in Protocol-1 and 2. Soluble iron concentration in
 88 raw water = $758 \pm 23.9 \mu\text{g L}^{-1}$. Error reflects the standard deviation in measurements of
 89 independent triplicate tests.

90 3. References

- 91 1. EPA US. Drinking Water Health Advisory for Manganese. US Environ Prot Agency Off
 92 Water. 2004;1–49.
- 93 2. NHMRC (National Health and Medical Research Council). Australian Drinking Water
 94 Guidelines 6 2011 [Internet]. National Health and Medical Research Council, National
 95 Resource Management Ministerial Council, Commonwealth of Australia,. 2011. 1244
 96 p. Available from:
 97 [https://www.nhmrc.gov.au/_files_nhmrc/file/publications/nhmrc_adwg_6_february_20](https://www.nhmrc.gov.au/_files_nhmrc/file/publications/nhmrc_adwg_6_february_2016.pdf)
 98 16.pdf

- 99 3. Who. Manganese in Drinking-water. Backgr Doc Dev WHO Guidel Drink water Qual.
100 2011;1–21.
- 101 4. Huber SA, Balz A, Abert M, Pronk W. Characterisation of aquatic humic and non-humic
102 matter with size-exclusion chromatography - organic carbon detection - organic nitrogen
103 detection (LC-OCD-OND). Water Res. 2011;45(2):879–85.
- 104 5. Huber SA, Balz A, Abert M, Pronk W. Characterisation of aquatic humic and non-humic
105 matter with size-exclusion chromatography–organic carbon detection–organic nitrogen
106 detection (LC-OCD-OND). Water Res. 2011;45(2):879–85.
- 107 6. Parker DS, Kaufman WJ, Jenkins D. Floc breakup in turbulent flocculation processes. J
108 Sanit Eng Div. 1972;98(1):79–99.
- 109